Bulletin of Electrical Engineering and Informatics
Vol. 13, No. 3, June 2024, pp. 1656~1666
ISSN: 2302-9285, DOI: 10.11591/eei.v13i3.7521

Compact dual-band antenna design for sub-6 GHz 5G application

Mahesh Kadu[1], Ramesh Pawase[1], Pankaj Chitte[2], Vilas S. Ubale[3]
[1]Departmentof Electronics and Telecommunication Engineering, Amrutvahini College of Engineering, Maharashtra, India
[2]Department of Electronics and Computer Engineering, Pravara Rural Engineering College, Maharashtra, India
[3]Department of Electronics and Computer Engineering, Amrutvahini College of Engineering, Maharashtra, India

Article Info

Article history:

Received Sep 6, 2023
Revised Oct 20, 2023
Accepted Mar 20, 2024

Keywords:

5G
Antenna
Antenna-gain
Compact
Dual-band

ABSTRACT

A design of a compact dual-band antenna for 5G application is presented in this research article. The dual-band operation includes the 3.6 GHz and 5.4 GHz frequency bands of the sub-6 GHz frequency band for 5G technology. The proposed antenna offers a compact design with satisfactory antenna performance parameters. Moreover, the dual-band antenna showcases the independent tuning ability for both frequency bands. The prototype of the dual-band antenna is manufactured and when tested for various antenna performance parameters shows a good agreement between the simulated and measured results. The proposed dual-band antenna has compact dimensions along with a peak gain of 2.2 dB and antenna efficiency of more than 90%.The antenna performance parameters are also compared with various dual-band antenna designs from the literature. The proposed dual-band antenna offers a compact design with satisfactory performance parameters and outperforms its counterparts.

Corresponding Author:

Mahesh Kadu
Department of Electronics and Telecommunication Engineering, Amrutvahini College of Engineering
Sangamner, Maharashtra, India
Email: mahesh.kadu@gmail.com

1. INTRODUCTION

5G is an emerging technology in the field of wireless communication. 5G devices support multiple wireless applications. A single-band antenna can support only a single wireless application designed for a given resonant frequency. To meet the need for an antenna for these multi-application 5G wireless devices, the antenna should be designed as a multi-resonant antenna [1]. The dual-band antenna is considered a possible solution for 5G wireless devices [2]. Also, a compact 5G device with multiple wireless applications has very little space for antenna elements [3]. Hence, it requires designing a compact dual-band antenna satisfying the key parameters such as return loss, gain, and radiation pattern. The dual-band antenna is developed in many ways as reported in the literature. A folded dipole dual-band antenna with rogers substrate was reported in [4]. The large size of the folded dipole antenna makes it unsuitable for 5G applications. The fractal geometry of the patch elements is a popular method to generate a dual-band resonance [5]-[7]. The consecutive iterations in the fractal design generate additional resonant frequencies converting a single-band design into a dual-band operation. However, fractal geometry may generate undesired resonant frequency bands and also lack independent tuning of individual bands. The antenna embedded with a split ring resonator yields a dual-band application [8]. The individual patch elements can be connected to form a dual band antenna with an independent tuning as reported in [9]. However, the size of the antenna increases with the addition of each patch. A dual-band resonance is obtained by truncating the corners of the patch as reported in [10]. The coplanar waveguide feeding method results in a dual-band operation of a rectangular

patch as investigated in [11]. A coplanar waveguide feeding experiences higher losses compared to other feeding techniques. The meta-material-based dual-band antenna is reported in [12]-[14]. Metamaterials are not readily available to the researcher which has led to its limited use in antenna design. The dual-band antenna design with a frequency-selective surface (FSS) is presented in [15]. The design process of an FSS-based antenna is quite complex and difficult to replicate. Luo *et al*. [16], gives a T-shaped dual-band antenna for sub-6 GHz 5G technology. The stack arrangement of parasitic patch elements yields a dual-band antenna as verified in [17]-[19]. The stack design increases the antenna dimensions in a vertical direction making it unsuitable for compact 5G wireless devices. A dual-band was realized by introducing slots in patch elements in [20], [21]. The slot in the patch may reduce the gain of the antenna. A monopole antenna was converted to a dual-band antenna [22], [23]. It's very difficult to achieve the exact resonance frequency bands with a monopole design. The reported dual-band antennas in the literature are larger in size. Also, they have a complex design technique. Moreover, most of them lack the independent tuning of individual frequency bands. All these factors make them unsuitable for 5G wireless applications.

The proposed work reports the design of a compact dual-band antenna with an economical FR4 substrate to support the dual frequency bands for sub-6 GHz 5G technology. A ground slot and a stub are designed to yielda dual-band operation at 3.6 GHz and 5.4 GHz frequency bands. The proposed design makes independent tuning possible for both bands. Also, the antenna is manufactured with an economical readily available FR4 dielectric substrate. Initially, an antenna with single frequency resonance is designed at a 5.4 GHz frequency band. The single frequency resonating antenna is converted to a dual-band antenna by adding a stub to generate additional resonance at 3.6 GHz. A detailed method for the research work is presented in section 2. Section 3 presents the design of a single-band antenna. The conversion of single-band operation to dual-band is presented in section 4. Results obtained from testing of the proposed antenna prototype are discussed in section 5. The concluding remarks of the research are presented in section 6.

2. METHOD

The method applied for the design and testing of the proposed compact dual-band antenna is demonstrated in Figure 1. A dual-band antenna for a given desired frequency band can be obtained by following the design steps. It will serve as a guideline for the researchers to replicate the dual-band antenna for other frequency bands.

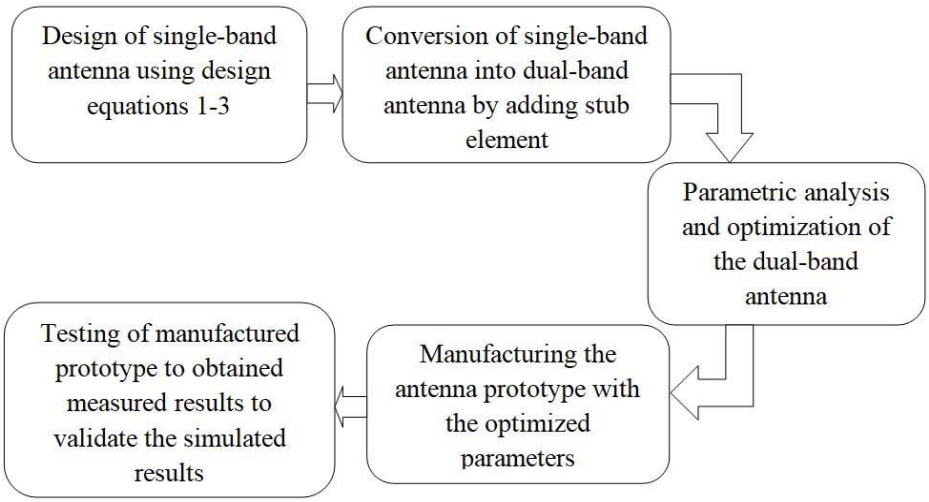

Figure 1. Method to design and manufacture proposed dual-band antenna

Step 1: a patch antenna is designed to resonate at a frequency that is higher than the two resonant frequencies selected for the dual-band operation and dielectric substrate using design (1)-(3).
Step 2: the single-band antenna is converted to a dual-band antenna by generating an additional resonance by adding a stub element of length obtained from (4).
Step 3: high-frequency structure simulator (HFSS) was used to carry out the parametric analysis of the proposed dual-band antenna. The antenna performance was evaluated against key parameters such as gain of the antenna, radiation pattern of the antenna element, and its return loss [24].

Step 4: the dual-band antenna showcasing excellent performance was manufactured using the given dielectric substrate.
Step 5: the validation of the simulated results was conducted by testing the manufactured prototype of the dual-band antenna in an antenna test facility.

3. SINGLE-BAND ANTENNA

At first, a basic single-band microstrip patch antenna fed by a microstrip line resonating at 5.4 GHz frequency designed with the design (1)-(3) on an economical FR4 substrate having a dielectric constant (ε_r)=4.4, and of height (h)=1.6 mm. The single-band antenna has a patch of length (L_p)=14 mm and width (W_p)=7 mm etched on an economical FR4 dielectric substrate of height=1.6 mm as seen in Figure 2(a). The substrate is of length (L_s)=20 mm and width (W_s)=20 mm. The ground structure of length (G_L)=20 mm and width (G_w)=20 mm is etched on the plane of the substrate opposite to the patch, as depicted in Figure 2(b). The optimized microstrip feed with width (W_f)=2 mm and length (L_f)=6.5 mm is etched on the same plane as that of the patch and is used to feed signal to the patch element through the input port. The patch width is obtained from design (1), (2) is used to obtain the effective dielectric constant (ε_{reff}), and the patch length is obtained from design (3) reported in [25]:

$$W_p = \frac{C}{2.f_r\sqrt{\frac{\varepsilon_r+1}{2}}} \quad (1)$$

Where C is the speed of light in free space.

$$L_p = \frac{C}{2.f_r\sqrt{\varepsilon_{reff}}} \quad (2)$$

$$\varepsilon_{reff} = \frac{\varepsilon_r+1}{2} + \frac{\varepsilon_r-1}{2}\frac{1}{\sqrt{1+12\frac{h}{W_p}}} \quad (3)$$

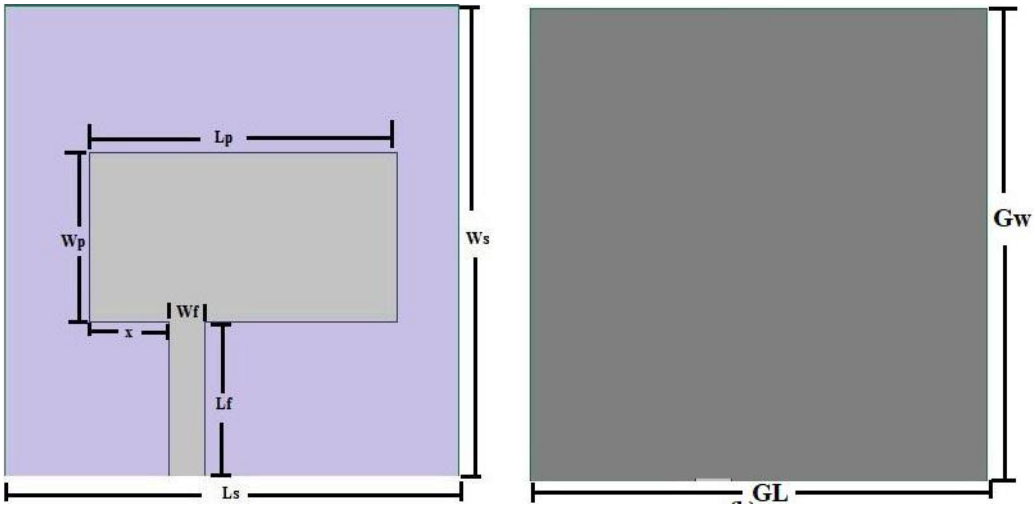

Figure 2. Single-band antenna; (a) top view and (b) bottom view

3.1. Parametric analysis of single-band antenna

The antenna resonance variation with the length of the patch (Lp) and its width (Wp) is presented in Figure 3. The antenna resonanceshifts to lower frequency with an increase in length of the patch from 12 to 15 mm, as illustrated in Figure 3(a). The antenna resonance shows a similar variation with the patch width, as seen in Figure 3(b). However, the antenna resonance varies more with the patch length than its width. Thus, the patch length plays a crucial role in optimizing the resonant frequency of the microstrip line-fed antenna at a 5.4 GHz frequency.

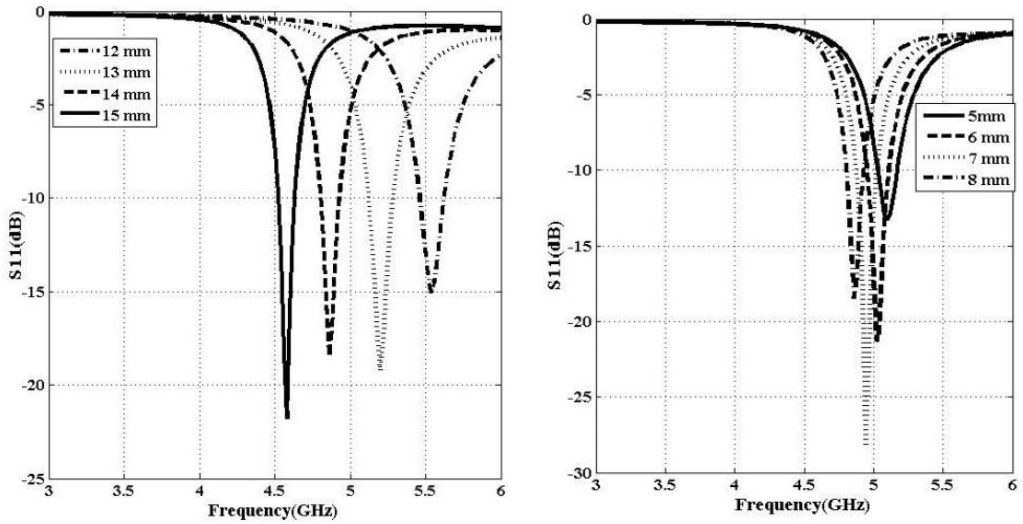

(a) (b)

Figure 3. Variation in single-band antenna resonance; (a) with patch length and (b) with patch width

4. COMPACT DUAL-BAND ANTENNA

The single-band designed in section 3 was converted to the compact dual-band antenna by adding a stub element as seen in Figure 4. The dual-band operation was further optimized by a patch slot and a ground slot below the stub element. This section covers the detailed design process and optimization of the compact dual-band antenna.

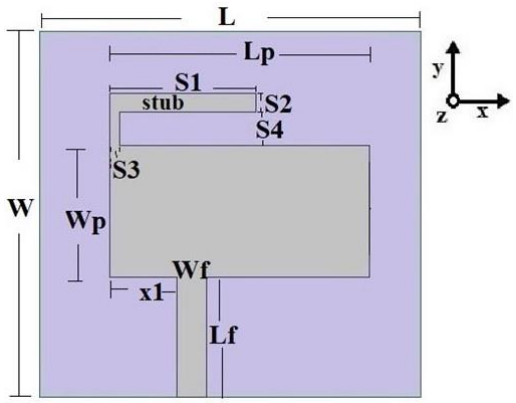

Figure 4. Dual-band antenna with stub

4.1. Dual-band antenna with stub

The single-band microstrip patch antenna resonates at 5.4 GHz. The single-band antenna was then converted into a dual-band by adding a stub of length 9 mm calculated from (4). The stub is placed on the patch where the current distribution is minimum at the 5.4 GHz frequency band. The stub increases the length of the patch antenna's current path, resulting in the generation of additional resonance at 3.6 GHz. The effect of the stub in generating a resonance at 3.6 GHz is visualized with the observation of the surface current distribution in the antenna, with a stub, at 3.6 GHz and 5.4 GHz, as seen in Figures 5(a) and (b), respectively. The surface current has moreconcentration in the stub element of the patch than in the rectangular patch element at 3.6 GHz, as seen in Figure 5(a). Figure 5(b) shows that the current is more in the rectangular patch than the stub at 5.4 GHz frequency. Thus, a dual-band antenna is achieved by embedding the stub in the single-band antenna structure as verified by Figure 5(c) showcasing resonance at two frequency bands as compared to single resonance for a single-band antenna without a stub. The dimensions of the dual-band antenna with stub are given in Table 1.

$$length\ of\ stub = \frac{C}{4.f_r} \quad (4)$$

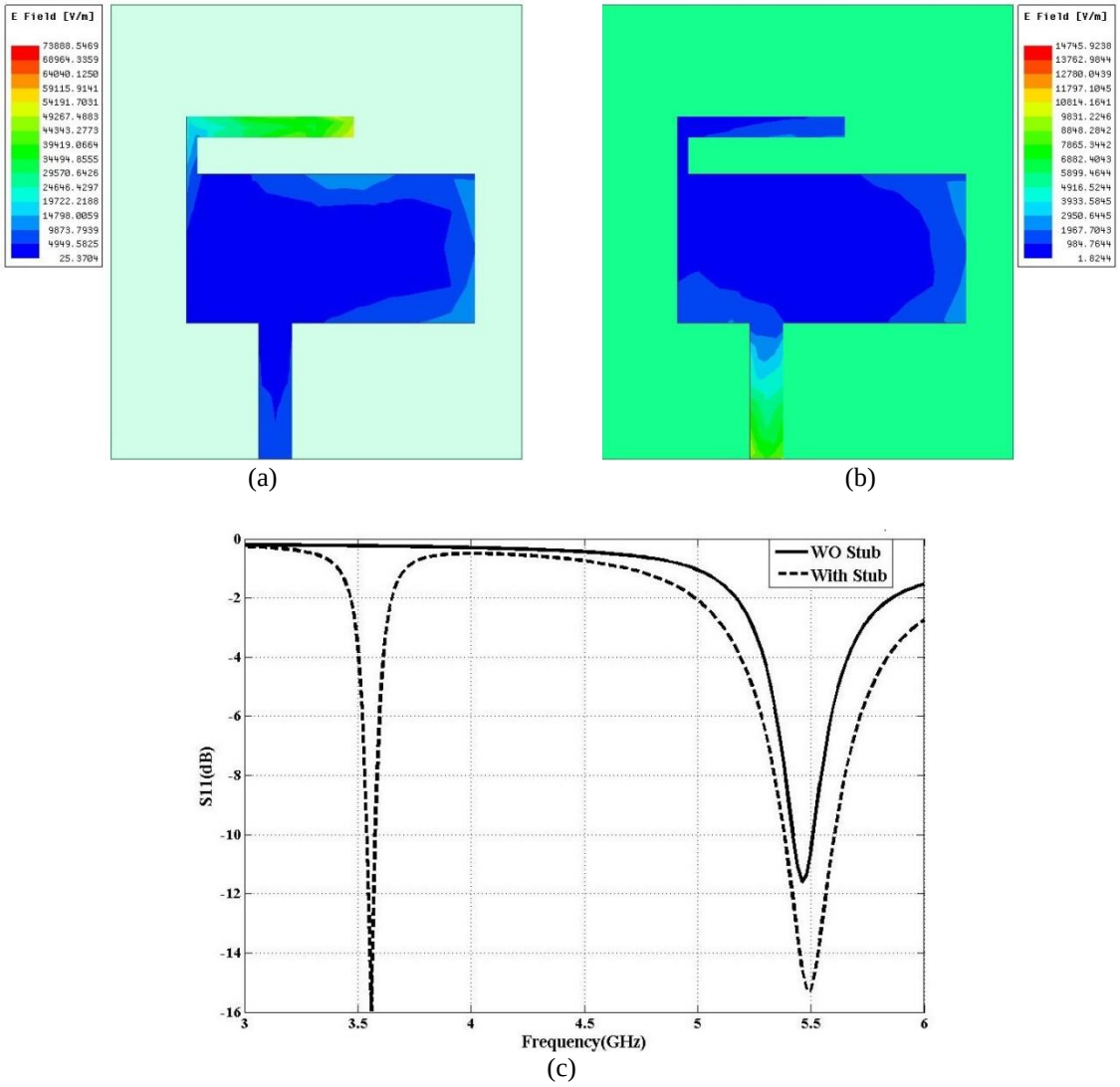

Figure 5. Dual-band antenna analysis; (a) distribution of surface current at 3.6 GHz, (b) distribution of surface current at 5.4 GHz, and (c) comparative resonance for single and dual-band antennas

Table 1. Optimized dimensions of dual-band antenna

Parameter	Wp	Lp	W	L	W_f	L_f	X_1	S_1	S_2	S_3	S_4	X_1
Dimensions(mm)	7	14	20	20	6.5	2	3.5	7	1	0.5	2	3.5

4.1.1. Parametric analysis of dual-band antenna with stub

A parametric analysis is conducted to investigate the independent tuning capability of the dual-band antenna at the 3.6 GHz frequency band. The findings of variation of the resonant frequency with horizontal stub arm width (S_2) are given in Figure 6. The 3.6 GHz resonance frequency varies with variation in S_2, while there are very few variations in the 5.4 GHz frequency band. Thus the 3.6 GHz frequency band can be independently tuned with the variation of S_2.

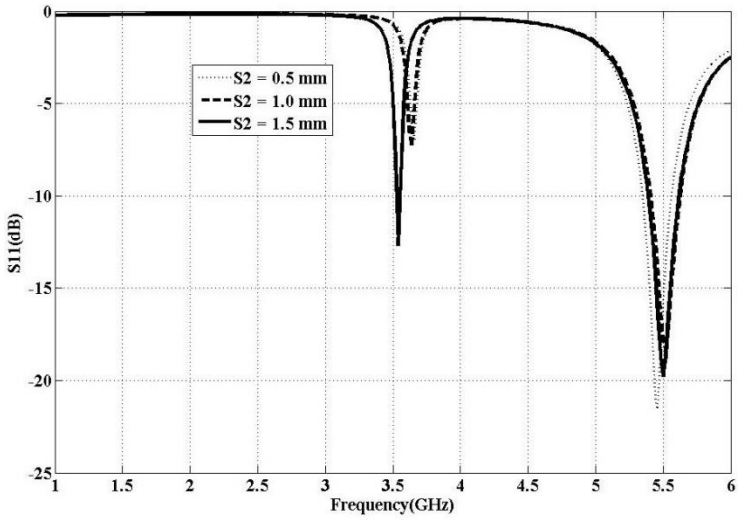

Figure 6. Independent tuning of 3.6 GHz frequency band

4.2. Dual-band antenna with stub, patch, and ground slot

The introduction of the stub shifts the resonance frequency to a 5.4 GHz band. Hence apatch slot of dimensions L_t=1.5 mmand W_t=4 mm as depicted in Figure 7(a) is created along the edge of the patch to fine tune the operating frequency of the antenna at 5.4 GHz. The operating frequency is optimized with variation in parameter W_t. To tune the antenna resonance at 5.4 GHz independently of 3.6 GHz a ground slot is created of dimensions Lg=13 mm and Wg=2.2 mm, as seen in Figure 7(b). The 5.4 GHz frequency band can be tuned independently with variation in ground slot width (Wg) as verified from the parametric analysis.

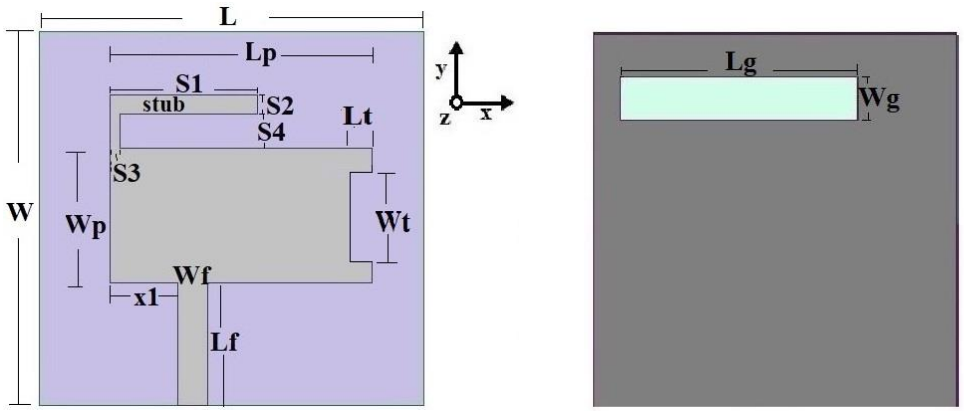

Figure7. Dual-band antenna with stub, patch, and ground slot; (a) top view displaying rectangular slot along the patch edge and (b) ground slot seen at the bottom of the antenna

4.2.1. Parametric analysis of dual-band antenna with patch, and ground slot

A parametric study of the effect of the patch slot parameter (W_t) and ground slot parameter (Wg) on the operating frequency of the dual-band antenna was carried out and the results are presented in Figure 8. A patch slot is created along the edge of the patch to optimize the operating frequency of the dual-band antenna at 5.4 GHz. It is seen in Figure 8(a) that the operating frequency at the 5.4 GHz band increases with parameter W_t. However, it also changes in a small amount at the 3.6 GHz frequency band.

A parametric analysis of variation of the resonant frequency with ground slot width (Wg) is presented in Figure 8(b). The 3.6 GHz resonance frequency remains entirely unaffected with variations in Wg, as seen in Figure 8(b). Thus, the ground slot enables the independent tuning of the 5.4 GHz frequency band.

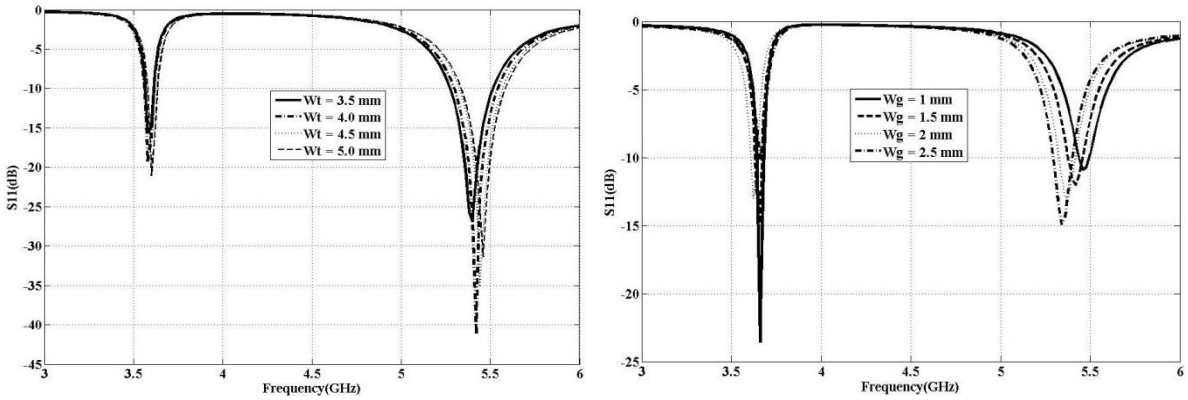

(a) (b)

Figure 8. Parametric analysis for; (a) antenna resonance with W_t and (b) antenna resonance with Wg of the ground slot

5. RESULTS AND DISCUSSION

The photograph of the manufactured proposed dual-band antenna is depicted in Figure 9. The top and bottom views of the manufactured antenna are seen in Figures 9(a) and (b), respectively. The reflection coefficient (S_{11}) of the prototype was measured with the help of the 2-port network analyzer setup. The simulated values were obtained using HFSS simulation software. The radiation pattern was tested in an anechoic chamber setup.

5.1. Return loss

The reflection coefficient at the input port was measured using a network analyzer. The measured return loss was compared with the simulated value as seen in Figure 9(c). The comparison plots show that the measured results match the simulated results at both frequencies. Small variations in the measured results can be attributed to manufacturing defects.

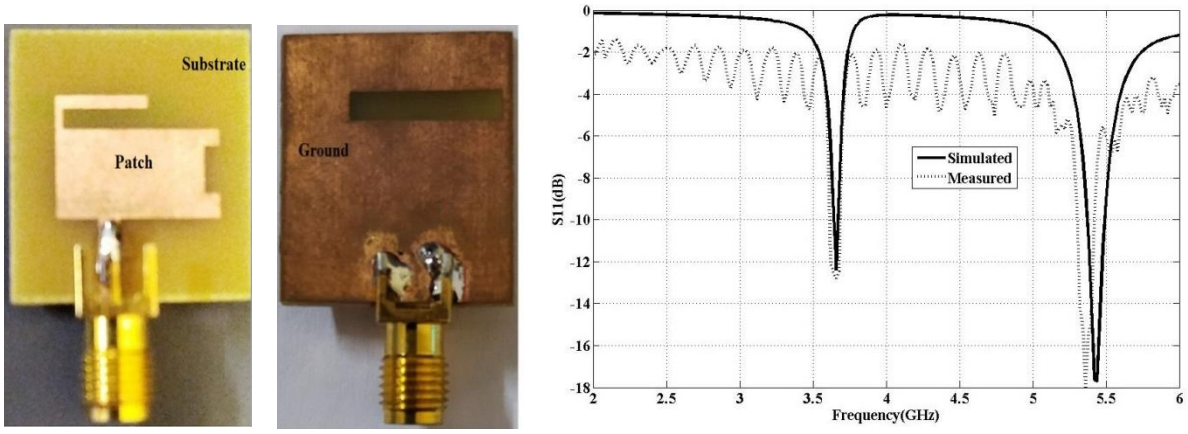

(a) (b) (c)

Figure 9. Prototype; (a) top view, (b) bottom view, and (c) return loss test results

5.2. Antenna gain and efficiency

The plot of gain and antenna efficiency is demonstrated in Figure 10. The proposed compact dual-band antenna exhibits a peak gain of 1.0 dB at 3.6 GHz frequency and 2.2 dB at 5.4 GHz frequency as depicted in Figures 10(a) and (b) respectively. The antenna efficiency obtained is around 86% at 3.6 GHz frequency and 91.2% at 5.4 GHz as depicted in Figure 10(c).

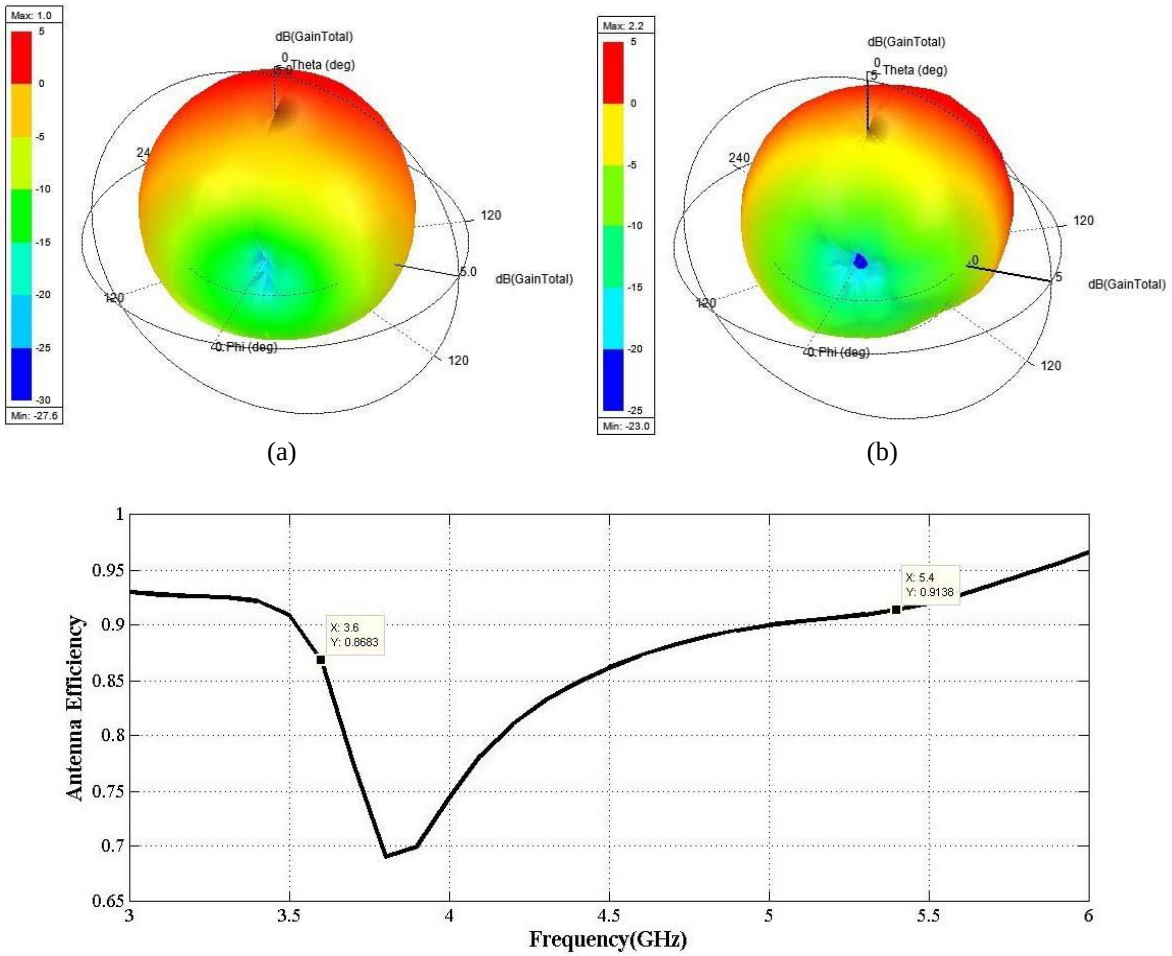

Figure 10. Peak gain of dual-band antenna; (a) at 3.6 GHz, (b) at 5.4 GHz, and (c) efficiency of dual-band antenna

5.3. Radiation pattern

The antenna radiation pattern of the dual-band antenna is plotted in Figure 11 (in Appendix). The plot in Figure 11(a) compares the simulated and measured E-plane (ϕ=0°) patterns of the dual-band antenna at 3.6 GHz frequency. Figure 11(b) depicts the comparative H-H-plane (ϕ=90°) radiation plot at 3.6 GHz. Figures 11(c) and (d) illustrate the E-plane and H-plane radiation plots, respectively, at 5.4 GHz. The plots show a stable radiation pattern at both frequencies. The anechoic chamber radiation pattern measurement setup is depicted in Figure 11(e).

5.4. Comparison of compact dual-band antenna with reported designs

The proposed compact dual-band antenna was compared with designs from the literature as given in Table 2. The proposed dual-band antenna offers a compact dual-band design compared to its counterparts. The gain and return loss values are satisfactory.

Table 2. Comparison of proposed dual-band antenna with existing designs

Ref.	Size	RL (dB)	Gain (dB)	Method	Tuning	Substrate
[4]	0.33 λ_0×0.33 λ_0	22	8	Multiple folded patch	Independent	Rogers RO4003
[9]	0.18 λ_0×0.21 λ_0	19	1.6	Connected patches	Independent	Metal
[11]	1.02 λ_0×1.02 λ_0	15	2.2	Modified feed	Non-independent	TLF-35A
[26]	0.25 λ_0×0.37 λ_0	17	1.9	Resonator	Non-independent	FR4
[5]	0.48 λ_0×0.48 λ_0	14	2.9	Fractal patch	Non-independent	FR4
[27]	0.12 λ_0×0.24 λ_0	20	1.4	Annular ring and U-shaped strip	Non-independent	FR4
[28]	0.4 λ_0×0.46 λ_0	17	Not reported	Slot loaded	Non-independent	FR4
Proposed	0.24 λ_0×0.24 λ_0	18	2.2	Stub	Independent	FR4

6. CONCLUSION

This work has resulted in the development of a dual-band antenna at 3.6 GHz and 5.4 GHz frequencies for sub-6 GHz 5G technologies. The proposed antenna offers a compact design with an economical FR4 dielectric substrate. The two frequency bands can be independently tuned with respect to each other. The 3.6 GHz frequency band can be tuned with the help of a variation of stub length. While the tuning of the 5.4 GHz frequency band is possible with a variation of ground slot. Thus, the design can be independently tuned to different frequencies in both of the frequency bands. The manufactured prototype was tested for various performance parameters. The return loss value obtained at 3.6 GHz and 5.4 GHz is more than 10 dB indicating a good impedance match. The proposed dual-band antenna exhibits a peak gain of 1 dB at 3.6 GHz and 2.2 dB at 5.4 GHz frequency. The antenna efficiency obtained at 3.6 GHz frequency is more than 86% and is about 91% at 5.4 GHz frequency. It shows a stable radiation pattern in both the frequency bands of operation. The measured results match with the simulated results. The antenna also shows better performance than various dual-band designs available in the literature.

APPENDIX

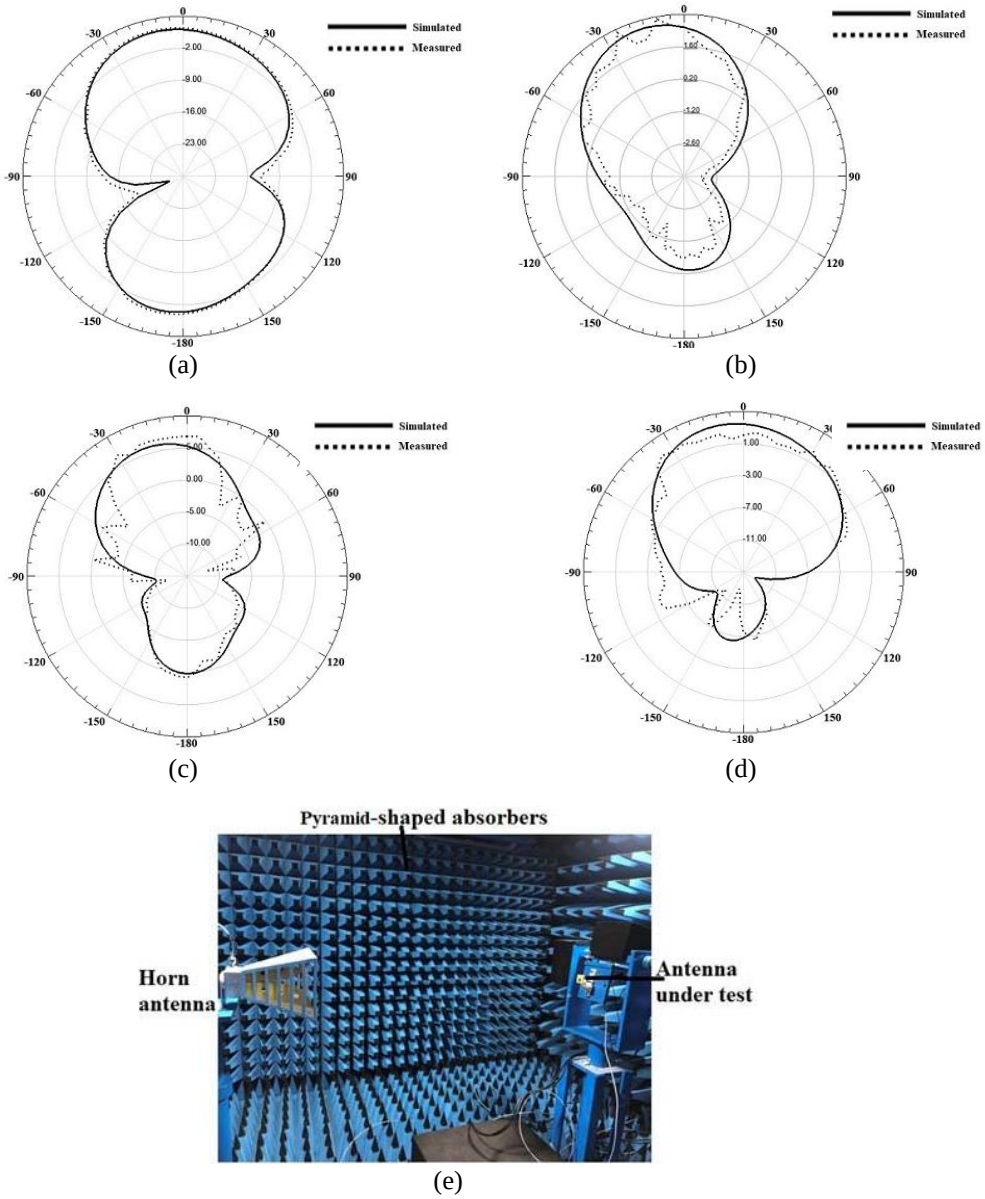

Figure 11. Radiation pattern of dual-band antenna at; (a) 3.6 GHz (E- plane), (b) at 3.6 GHz (H- plane), (c) at 5.4 GHz (E- plane), (d) at 5.4 GHz (H- plane), and (e) anechoic radiation pattern setup

REFERENCES

[1] U. Illahi *et al.*, "A Novel Design and Development of a Strip-Fed Circularly Polarized Rectangular Dielectric Resonator Antenna for 5G NR Sub-6 GHz Band Applications," *Sensors*, vol. 22, no. 15, pp. 1–16, 2022, doi: 10.3390/s22155531.

[2] I. Bari *et al.*, "Bandwidth Enhancement and Generation of CP of Yagi-Uda-Shape Feed on a Rectangular DRA for 5G Applications," *Micromachines*, vol. 13, no. 11, p. 1913, 2022, doi: 10.3390/mi13111913.

[3] Y. Li, C. Y. D. Sim, Y. Luo, and G. Yang, "Multiband 10-Antenna Array for Sub-6 GHz MIMO Applications in 5-G Smartphones," *IEEE Access*, vol. 6, pp. 28041–28053, 2018, doi: 10.1109/ACCESS.2018.2838337.

[4] X. Liu *et al*., "A Mutual-Coupling-Suppressed Dual-Band Dual-Polarized Base Station Antenna Using Multiple Folded-Dipole Antenna," in *IEEE Transactions on Antennas and Propagation*, vol. 70, no. 12, pp. 11582-11594, Dec. 2022, doi: 10.1109/TAP.2022.3209177.

[5] N. L. Nhlengethwa and P. Kumar, "Fractal microstrip patch antennas for dual-band and triple-band wireless applications," *International Journal on Smart Sensing and Intelligent Systems*, vol. 14, no. 1, pp. 1–9, 2021, doi: 10.21307/IJSSIS-2021-007.

[6] N. S. Dandgavhal, M. B. Kadu, and R. P. Labade, "Design and simulation of Koch Snowflake fractal antenna for GPS, WiMAX and radar application," in *2015 IEEE Bombay Section Symposium: Frontiers of Technology: Fuelling Prosperity of Planet and People, IBSS 2015*, 2015, pp. 1-5, doi: 10.1109/IBSS.2015.7456659.

[7] S. Shrestha, S. R. Lee, and D. Y. Choi, "A new fractal-based miniaturized dual band patch antenna for RF energy harvesting," *International Journal of Antennas and Propagation*, vol. 2014, 2014, doi: 10.1155/2014/805052.

[8] Z. Xu, Q. Zhang, and L. Guo, "A compact 5G decoupling MIMO antenna based on split-ring resonators," *International Journal of Antennas and Propagation*, vol. 2019, 2019, doi: 10.1155/2019/3782528.

[9] J. Guo, H. Bai, A. Feng, Y. Liu, Y. Huang and X. Zhang, "A Compact Dual-Band Slot Antenna With Horizontally Polarized Omnidirectional Radiation," in *IEEE Antennas and Wireless Propagation Letters*, vol. 20, no. 7, pp. 1234-1238, July 2021, doi: 10.1109/LAWP.2021.3076169.

[10] F. I. Alnemr, M. F. Ahmed, and A. A. Shaalan, "Dual-Band Circularly Polarized Mobile Antenna for Millimeter-Wave Antenna Applications," *Journal of Physics: Conference Series*, vol. 1447, no. 1, 2020, doi: 10.1088/1742-6596/1447/1/012013.

[11] H. Liu, L. Meng, X. Huo and S. Liu, "A Cpw-fed Dual-Band Dual-Pattern Radiation Patch Antenna Based on TM01 and TM02 Mode," *2020 9th Asia-Pacific Conference on Antennas and Propagation (APCAP)*, Xiamen, China, 2020, pp. 1-2, doi: 10.1109/APCAP50217.2020.9245936.

[12] A. A. Ibrahim, M. A. Abdalla and R. M. Shubair, "High-isolation metamaterial MIMO antenna," *2017 IEEE International Symposium on Antennas and Propagation & USNC/URSI National Radio Science Meeting*, San Diego, CA, USA, 2017, pp. 1737-1738, doi: 10.1109/APUSNCURSINRSM.2017.8072911.

[13] M. Najumunnisa *et al.*, "A Metamaterial Inspired AMC Backed Dual Band Antenna for ISM and RFID Applications," *Sensors*, vol. 22, no. 20, p. 8065,2022, doi: 10.3390/s22208065.

[14] M. R. Islam, A. A. A. Adel, A. W. N. Mimi, M. S. Yasmin, and F. A. M. Norun, "Design of Dual Band Microstrip Patch Antenna using Metamaterial," *IOP Conference Series: Materials Science and Engineering*, vol. 260, no. 1, p. 012037, 2017, doi: 10.1088/1757-899X/260/1/012037.

[15] A. Chatterjee, S. Banerjee, J. Frnda, and M. Dvorsky, "Planar FSS Based Dual-Band Wire Monopole Antenna for Multi-Directional Radiation With Diverse Beamwidths," *IEEE Access*, vol. 10, pp. 30427–30435, 2022, doi: 10.1109/ACCESS.2022.3159337.

[16] C. M. Luo, J. S. Hong, and M. Amin, "Mutual coupling reduction for dual-band MIMO antenna with simple structure," *Radioengineering*, vol. 26, no. 1, pp. 51–58, 2017, doi: 10.13164/re.2017.0051.

[17] L. Chang and H. Liu, "Low-Profile and Miniaturized Dual-Band Microstrip Patch Antenna for 5G Mobile Terminals," in *IEEE Transactions on Antennas and Propagation*, vol. 70, no. 3, pp. 2328-2333, March 2022, doi: 10.1109/TAP.2021.3118730.

[18] J. A. Ansari, P. Singh, S. K. Dubey, R. U. Khan, and B. R. Vishvakarma, "H-shaped stacked patch antenna for dual band operation," *Progress In Electromagnetics Research B*, vol. 5, pp. 291–302, 2008, doi: 10.2528/pierb08031203.

[19] M. K. Khandelwal, B. K. Kanaujia, S. Dwari, S. Kumar, and A. K. Gautam, "Analysis and design of dual band compact stacked microstrip patch antenna with defected ground structure for WLAN/WiMAX applications," *AEU - International Journal of Electronics and Communications*, vol. 69, no. 1, pp. 39–47, 2015, doi: 10.1016/j.aeue.2014.07.018.

[20] X. Zhang, Z. Teng, Z. Liu, and B. Li, "A dual band patch antenna with a pinwheel-shaped slots EBG substrate," *International Journal of Antennas and Propagation*, vol. 2015, 2015, doi: 10.1155/2015/815751.

[21] S. Ahmad, A. Ghaffar, N. Hussain, and N. Kim, "Compact dual-band antenna with paired l-shape slots for on-and off-body wireless communication," *Sensors*, vol. 21, no. 23, p. 7953, 2021, doi: 10.3390/s21237953.

[22] H. Zhai, Q. Gao, Z. Ma, and C. Liang, "Dual Y-shaped monopole antenna for dual-band WLAN/WiMAX operations," *International Journal of Antennas and Propagation*, vol. 2014, 2014, doi: 10.1155/2014/481918.

[23] P. Jithu, A. Paul, V. Pithadia, R. Misquitta, and U. P. Khot, "Dual band monopole antenna design," *International Journal of Engineering and Technology (IJET)*, vol. 5, no. 3, pp. 2297–2302, 2013.

[24] Ansoft Corporation, "User's guide–High Frequency Structure Simulator," p. 801, 2005, [Online]. Available: http://anlage.umd.edu/HFSSv10User Guide.pdf (accessed 03-02-2023).

[25] G. Kumar and K. P. Ray, "An Introduction to Microstrip Antenna," *Broadband Microstrip Antennas Handb.*, pp. 1–20, 2003.

[26] M. Aminu-Baba *et al.*, "Compact Patch MIMO Antenna With Low Mutual Coupling For WLAN Applications," *ELEKTRIKA-Journal of Electrical Engineering*, vol. 18, no. 1, pp. 43–46, Apr. 2019, doi: 10.11113/ELEKTRIKA.V18N1.146.

[27] A. Khade, M. A. Trimukhe, S. M. Verulkar, and R. K. Gupta, "Dual Band MIMO Antenna with High Isolation for GSM and WLAN Applications," *Progress In Electromagnetics Research C*, vol. 136, pp. 189–198, 2023, doi: 10.2528/PIERC23060104.

[28] M. C. Borah, P. Saikia, A. K. Bordoloi, and B. Sarma, "Slot Loaded Microstrip Triangular Patch Antenna for dual frequency applications in S band," *Journal of Positive School Psychology*, vol. 6, no. 3, pp. 4326–4332, 2022.

BIOGRAPHIES OF AUTHORS

Dr. Mahesh Kadu completed his graduation in Electronics and Telecommunication Engineering from Pravara Rural Engineering College (PREC) of Savitribai Phule University, India in 2006, and M.Tech. in Electronics and Telecommunication Engineering Dr.BATU in 2011. He was awarded a Ph.D. by Symbiosis International University, India. His research interests are primarily in the area of wireless communications and networks. He can be contacted at email: mahesh.kadu@gmail.com.

Dr. Ramesh Pawase received a B.E. in Electronics Engineering and M.Tech. Department of Electronics and Telecommunication Engineering from Amrutvahini College of Engineering, Sangamner and Dr. BATU, India, in 2004 and 2009 respectively, and the Ph.D. degree in Department of Electronics and Telecommunication Engineering from SPPU,Pune, India in 2019. Currently, he is an Associate Professor at the Department of Electronics and Telecommunication Engineering, Amrutvahini College of Engineering, Sangamner, M.S., India. He is a member of the board of studies, at SPPU and a Research Guide in Department of Electronics and Telecommunication Engineering. His research interests include MEMS sensors, CMOS-ASIC, and power electronics. He can be contacted at email: rameshpawase@gmail.com.

Dr. Pankaj Chitte received a Bachelor of Engineering in Electronics and Telecommunication from SPPU, Pune, India, and a Master of Engineering in Electronics Engineering, from Dr. BAMU, Aurangabad, India, and Ph.D. in Electronics Engineering from RashtrasantTukdoji Maharaj University, Nagpur India. Currently, he is the Assistant Professor of the Electronics and Computer Engineering Department of Pravara Rural Engineering College Loni, India. He can be contacted at email: chittepp@pravaraengg.org.in.

Dr. Vilas S. Ubale did a B.E in Electronics and Telecommunication Engineering from Amravati University in 2002, an M.E in Electronics Engineering from Government College of Engineering, Aurangabad (B.A.M. University) in 2009, and a Ph.D. in Electronics and Communication Engineering from Suresh Gyan Vihar University Jaipur (Rajasthan) in June 2022. His research field area is microwave antenna design. He can be contacted at email: vilas.ubale@avcoe.org.